

Deep Learning for Image Analysis

Classification of Satellite Image Time Series with Transformers

Romain Thoreau
UMR MIA Paris-Saclay - EkiNocs Team
romain.thoreau@agroparistech.fr

January 16, 2026



Overview

Earth observation: a brief introduction

The Copernicus program

Optical imaging

Classification of irregular Sentinel-2 image time series with Transformers

Overview

Earth observation: a brief introduction

The Copernicus program

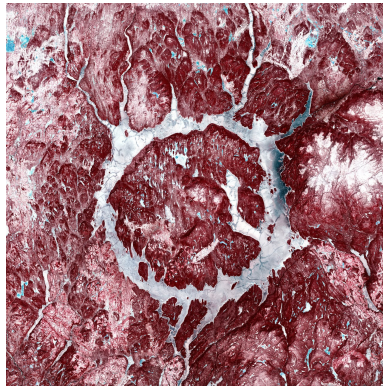
Optical imaging

Classification of irregular Sentinel-2 image time series with Transformers

Earth observation from space: the Copernicus program



(a) Antarctic Peninsula, modified Copernicus Sentinel-1 data (2025), processed by ESA.



(b) Manicouagan crater (Québec), modified Copernicus Sentinel-2 data (2022), processed by ESA.

Earth observation from space: the Copernicus program

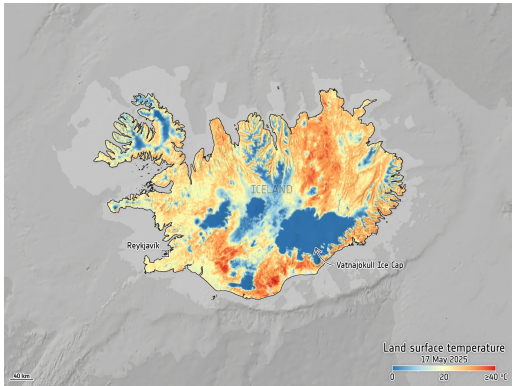
Figure: Flood in Puttalam district in North Western Sri Lanka, modified Copernicus Sentinel-2 data (2025), processed by ESA.

Figure: Yearly ice algal bloom onset dates from 2011 to 2022. CryoSat/Copernicus Sentinel-3/ICESat-2.

Earth observation from space: the Copernicus program



(a) Palisades fire (Los Angeles), modified Copernicus Sentinel-3 data (2025), processed by ESA.

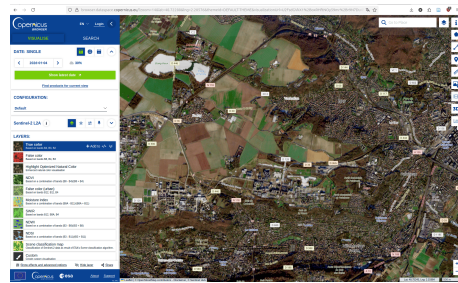


(b) 2025 heatwave in Iceland, modified Copernicus Sentinel-3 data (2025), processed by ESA.

Earth observation from space: the Copernicus program



(a) <https://www.copernicus.eu/fr>



(b) <https://browser.dataspace.copernicus.eu>

Overview

Earth observation: a brief introduction

The Copernicus program

Optical imaging

Classification of irregular Sentinel-2 image time series with Transformers

Spectral sensitivity of optical sensors: the Sentinel-2 case

- The detectors of an optical sensor are sensitive to the light energy (in joules) received during the measurement¹. Each detector are sensitive to a different part of the solar spectrum.

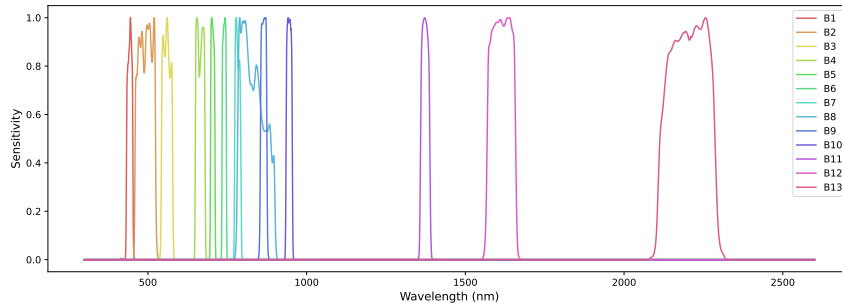


Figure: Spectral sensitivity of the Sentinel-2 sensor.

¹Further details at:

<https://www.cesbio.cnrs.fr/multitemp/radiometric-quantities-irradiance-radiance-reflectance/>

Energy and radiance

- The energy received by a detector, with sensitivity $S(\lambda)$ between $[\lambda_1, \lambda_2]$, during the observation is expressed as follows:

$$\epsilon_{detector} = \int_{\lambda_1}^{\lambda_2} S(\lambda) \epsilon(\lambda) d\lambda$$

where $\epsilon(\lambda)$ is the light spectral energy.²

- This energy is equal (up to a constant that depends on the sensor) to the spectral radiance $R_{[\lambda_1, \lambda_2]}$ averaged in the range $[\lambda_1, \lambda_2]$, that only depends on the observation. The spectral radiance is the spectral flux that reaches the instrument per unit area, per unit of solid angle, and per unit wavelength. It is measured in $\text{W/m}^2/\text{sr}/\mu\text{m}$.

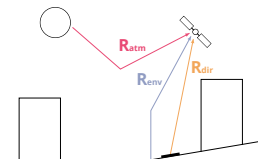


Figure: Illustration of the direct, environmental and atmospheric radiance terms.

²<https://www.cesbio.cnrs.fr/multitemp/radiometric-quantities-irradiance-radiance-reflectance/>

Surface reflectance

- In the spectral range [400 nm - 2500 nm], the radiance of the Earth surface comes from the reflection of the sun irradiance $I(\lambda)$ (W/m^2), that depends on the time, day of year, atmospheric conditions, and topography.

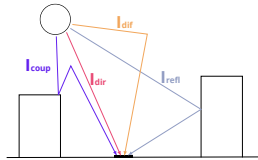


Figure: Illustration of the direct, diffuse, reflected and coupled irradiance terms.

- Therefore, we are interested in the reflectance, that only depends on the surface chemical properties³:

$$\rho(\lambda) = \frac{\pi R(\lambda)}{I(\lambda) \cos \theta_s}$$

where θ_s is the solar zenith angle (the angle between the solar direction and the normal of the surface).

³We assume that the surface is lambertian, i.e., that it does not depend on the solar direction neither the observation direction.

Atmospheric correction: from top-of-atmosphere to bottom-of-atmosphere reflectance

- ▶ Atmospheric correction codes, e.g. MAJA (CNES / CESBIO), correct the measured signal from atmospheric effects such as the absorption and scattering of water vapor.



(a) L1C level: Top-of-Atmosphere (TOA) reflectance data



(b) L2A level: Bottom-of-Atmosphere (BOA) reflectance data

Figure: Sentinel-2 images over Provence-Alpes-Côte-d'Azur. Credit: Copernicus, ESA, CNES.

Hyperspectral and multispectral imaging: application to vegetation monitoring

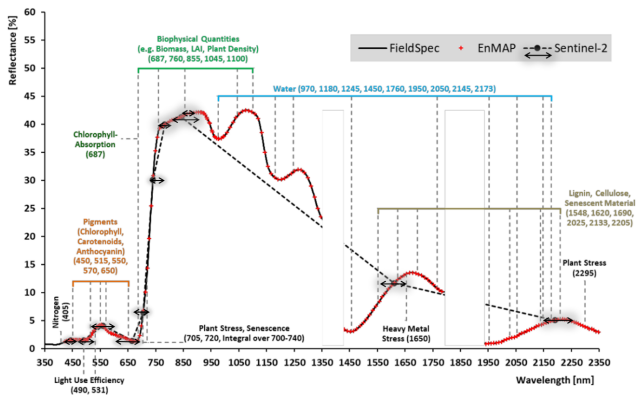


Figure: Spectral response of vegetation for a hyperspectral sensor (EnMAP) and multispectral sensor (Sentinel-2). Source: [Laroche-Pinel, 2021].

Overview

Earth observation: a brief introduction

The Copernicus program

Optical imaging

Classification of irregular Sentinel-2 image time series with Transformers

Sentinel-2 image time series of agricultural crops

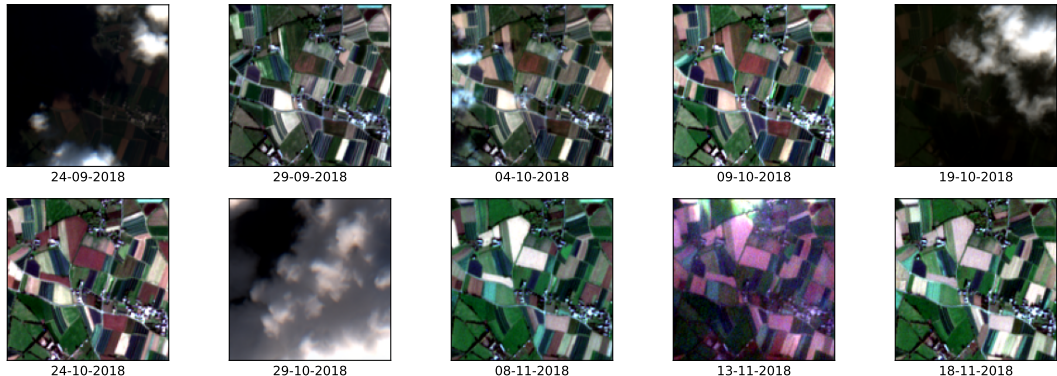


Figure: Sample of the PASTIS dataset [Sainte Fare Garnot and Landrieu, 2021] for crop type classification. Multispectral image time series are very useful in order to detect phenological phases, relevant for crop type classification. At some dates, the cloud cover masks the crops.

Satellite Image Time Series Classification with Pixel-Set Encoders and Temporal Self-Attention [Garnot et al., 2020]

- ▶ Transformers can naturally handle irregular time series.
- ▶ Can we process sequence of multispectral images like a sequence of words? Can you spot differences with respect to the traditional Transformer?

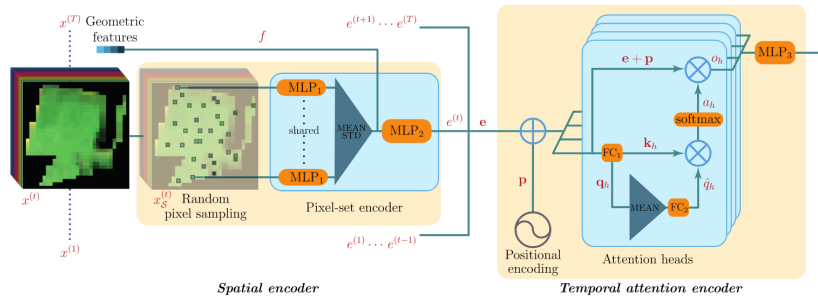


Figure: Schematic view of the spatio-temporal encoder introduced in [Garnot et al., 2020].

Try for yourself!

https://dl4ia.readthedocs.io/en/latest/tutorials/sits_classification/sits_classification.html



Garnot, V. S. F., Landrieu, L., Giordano, S., and Chehata, N. (2020).

Satellite image time series classification with pixel-set encoders and temporal self-attention.

In *Proceedings of the IEEE/CVF Conference on Computer Vision and Pattern Recognition*, pages 12325–12334.



Laroche-Pinel, E. (2021).

Suivi du statut hydrique de la vigne par télédétection hyper et multispectrale.

PhD thesis.



Sainte Fare Garnot, V. and Landrieu, L. (2021).

Panoptic segmentation of satellite image time series with convolutional temporal attention networks.

ICCV.